Stem Cell Reports, Volume *13*

Supplemental Information

A Chemically Defined Feeder-free System for the Establishment and Maintenance of the Human Naive Pluripotent State

Iwona Szczerbinska, Kevin Andrew Uy Gonzales, Engin Cukuroglu, Muhammad Nadzim Bin Ramli, Bertha Pei Ge Lee, Cheng Peow Tan, Cheng Kit Wong, Giulia Irene Rancati, Hongqing Liang, Jonathan Göke, Huck-Hui Ng, and Yun-Shen Chan

Supplementary Information.

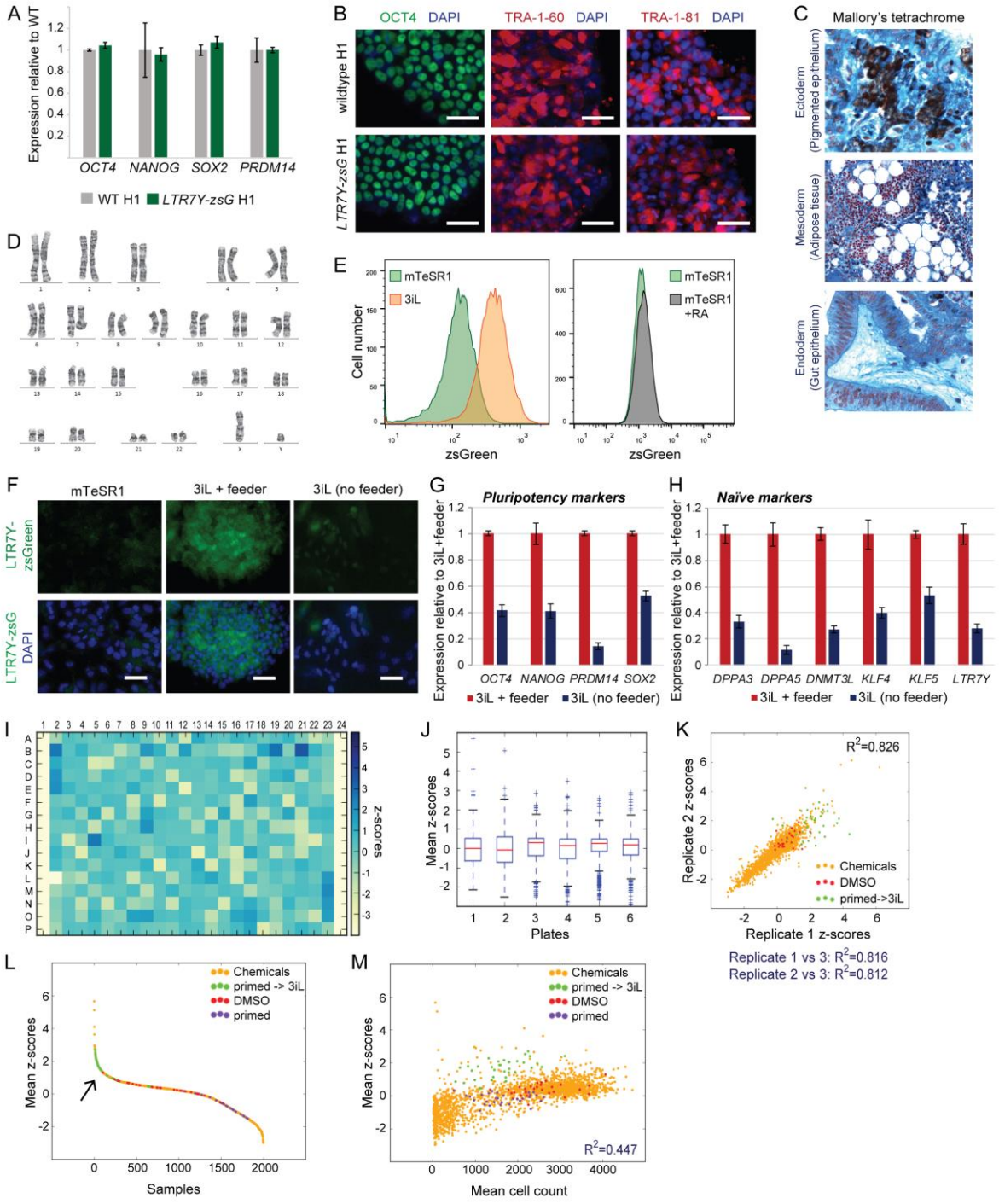

Figure S1. Validation of *LTR7Y-zsGreen* reporter and quality control of small molecule screen, related to Fig. 1.

(A) Gene expression analysis of pluripotency associated genes: *OCT4*, *NANOG*, *SOX2* and *PRDM14* in WT-H1 (parental line) and *LTR7Y-zsGreen* reporter line. Mean ± SD of three independent experiments.

(B) Immunofluorescence staining of pluripotency markers: OCT4, TRA-1-60, TRA-1-81 in WT-H1 (parental line) and *LTR7Y-zsGreen* reporter cells. Scale bar = 50 µm

(C) *LTR7Y-zsGreen* reporter cells give rise to teratomas consisting of cells from mesodermal, ectodermal and endodermal lineages.
(D) Cytogenetic analysis of *LTR7Y-zsGreen* reporter cells confirms normal karyotype.
(E) FACS analysis of *LTR7Y-zsGreen* reporter cells cultured in mTeSR1 (green), 3iL (orange) and mTeSR1 supplemented with retinoic acid (RA) culture conditions.
(F) Microscopy images showing induction of *LTR7Y-zsGreen* reporter activity in 3iL with feeder and 3iL without feeder culture conditions, compared to mTeSR1. Scale bar = 50 μm
(G-H) Gene expression analysis for **(G)** pluripotency markers and **(H)** naïve markers in 3iL culture with or without feeders. Mean ± SD of three independent experiments. RNA was collected after 6 days in culture.
(I) Representative heatmap for z-scores of one plate from 3iL screen. No plate layout bias is evident.
(J) Boxplots showing the alignment of plates after z-score normalisation for 3iL *LTR7Y-zsGreen* small molecule screen.
(K) Scatterplot showing correlation between replicates for 3iL screen. Pearson correlation values between replicates are indicated.
(L) Descending plot of screen samples. Inflection point (denoted by arrow) is below the chosen stringent cut-off of z-score >2. Most positive controls (primed -> 3iL) are above the inflection point.
(M) Representative dot plot of z-scores (y axis) versus cell count (x axis) from 3iL chemical screen. No significant correlation is observed.

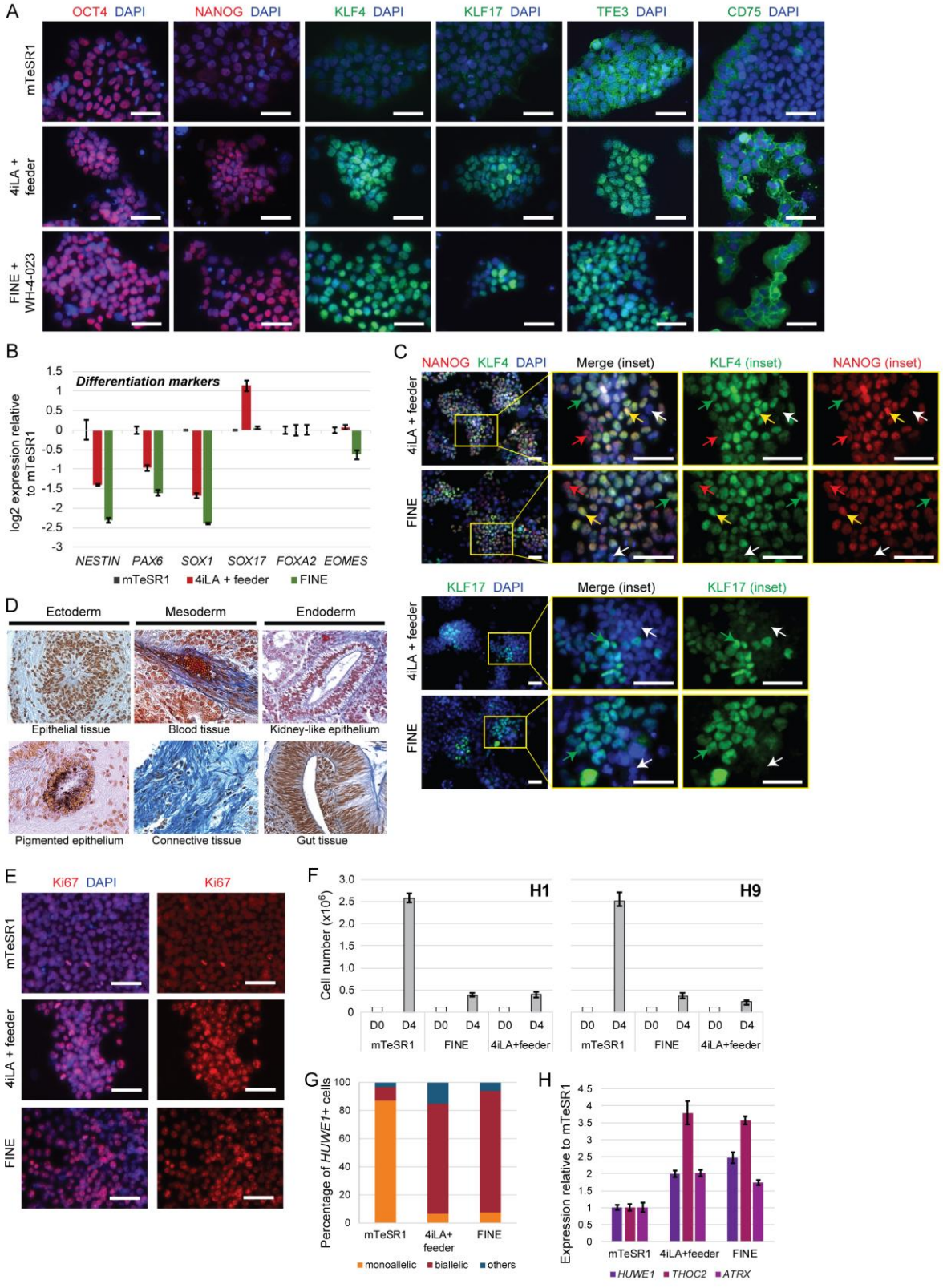

Figure S2. Supplementary to Figure 3.
(A) Immunofluorescence staining of OCT4, NANOG, KLF4, KLF17, TFE3 and CD75 in H1 cells cultured under mTeSR1, 4iLA+feeder and FINE+WH-4-023 conditions. Scale bar = 50 µm.

(B) Gene expression of lineage-specific markers in H1 cell culture under mTeSR1, 4iL+feeder and FINE conditions. Mean ± SD of three independent experiments.
(C) Side-by-side comparison of immunofluorescence staining of NANOG, KLF4 and KLF17 in H1 cells cultured under 4iLA+feeder and FINE conditions to demonstrate heterogeneity of expression in both naïve conditions. Arrows highlight representative cells that are positive in the green channel (green arrow), red channel (red arrow), both channels (yellow arrow) or negative for both channels (white arrow). Scale bar = 50 µm.
(D) FINE cultured cells give rise to teratomas consisting of cells from mesodermal, ectodermal and endodermal lineages.
(E) Immunofluorescence staining of Ki67 proliferation marker of hESCs under mTeSR1, 4iLA+feeder and FINE conditions. Scale bar = 50 µm.
(F) Measurement of proliferation rate of hESCs (H1 and H9) cultured in various conditions. 120,000 cells were seeded (D0 in white) and cell count was performed 4 days post-seeding (D4 in gray) at passage 8. Mean ± SD of three independent experiments.
(G) Quantification of percentage of *HUWE1*+ cells in hESCs under mTeSR1, 4iLA+feeder and FINE. Only cells showing biallelic *XACT* were included in the analysis. N=60 cells.
(H) qPCR analysis of transcripts from the X-chromosome in hESCs cultured under mTeSR1, 4iLA+feeder and FINE conditions, to determine X activation status. Mean ± SD of three independent experiments.

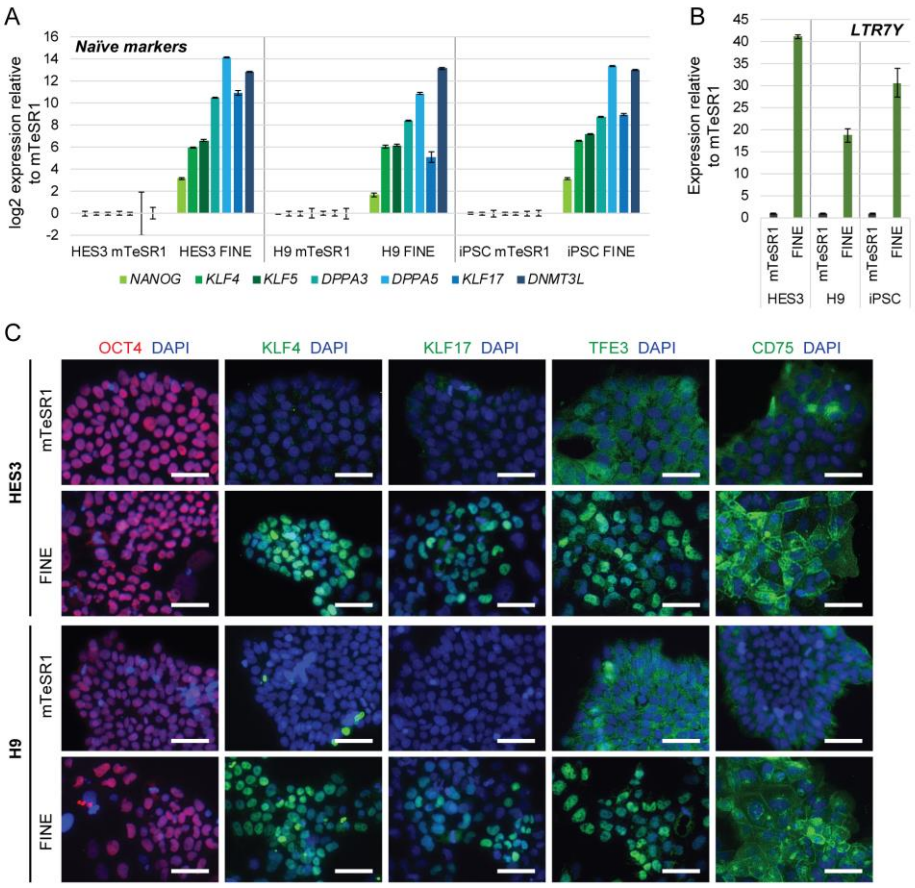

Figure S3. FINE culture is applicable to multiple human pluripotent cell lines, related to Fig. 3.

(A) Gene expression of naïve-associated genes in H9 and HES3 cell lines, and in the GM23338 iPSC line cultured under mTeSR1 and FINE conditions. Mean ± SD of three independent experiments.
(B) qPCR analysis of *LTR7Y* and *HERVH* in H9 and HES3 cells cultured under mTeSR1 and FINE conditions for H9, HES3 and iPSC lines. Mean ± SD of three independent experiments.
(C) Immunofluorescence staining of OCT4, KLF4, KLF17, TFE3 and CD75 in HES3 and H9 cells cultured under mTeSR1 and FINE conditions. Scale bar = 50 µm

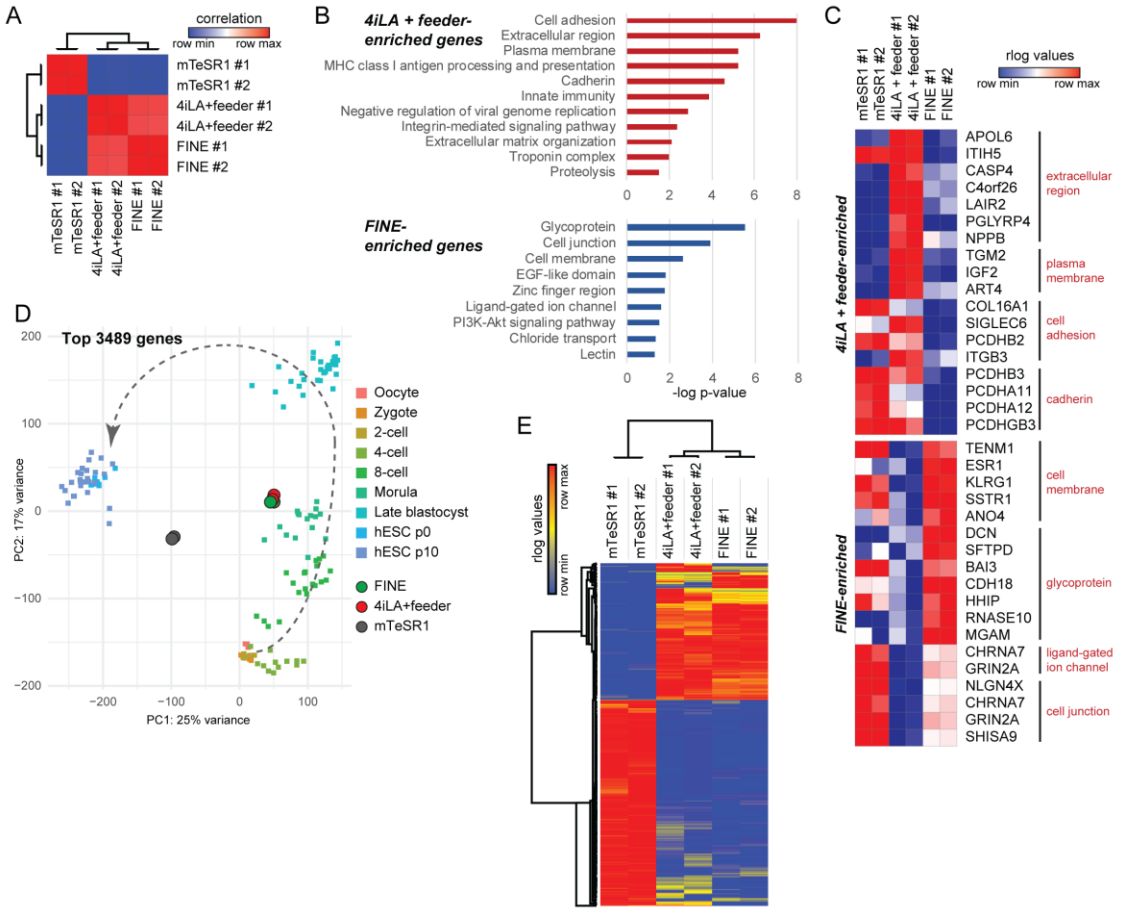

Figure S4. Supplementary to Figure 5.
(A) Hierarchical clustering based on top 1000 differentially expressed genes between mTeSR1, 4iLA+feeder and FINE cultured cells.
(B) Gene ontology analysis of terms enriched in 4iLA+feeder in comparison to FINE cultured cells and FINE enriched terms in comparison to 4iLA+feeder cultured cells.
(C) Representative genes from differentially expressed genes between 4iLA+feeder and FINE cultures presented in heatmaps grouped based on putative roles (by gene ontology).
(D) PCA plot based on the top 3489 genes differentially expressed across conditions. Single cell *in vivo* embryonic data (Yan et al., 2013) are represented as squares, while FINE, 4iLA+feeder and mTeSR1 from our bulk RNA-seq data are drawn as circles.
(E) Heatmap of RNA-seq expression data based on top 1000 differentially expressed transposable elements between mTeSR1, 4iLA+feeder and FINE cultured cells.

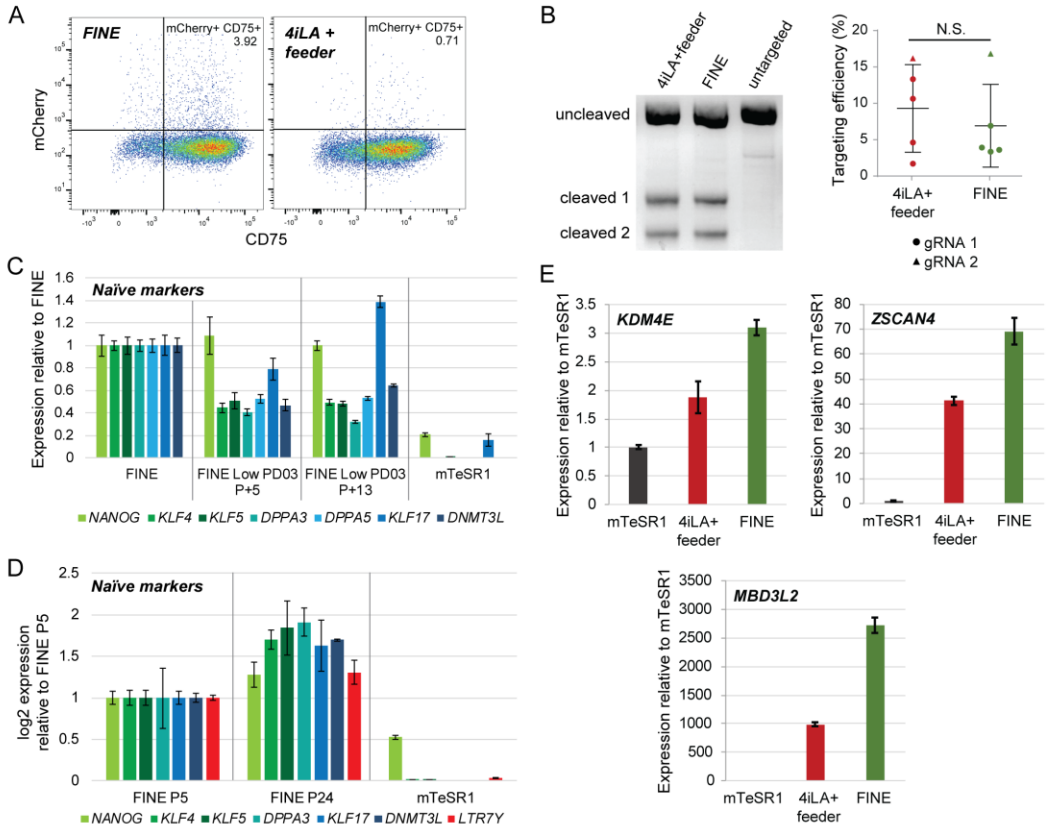

Figure S5. Supplementary to Figure 7.

(A) Representative FACS gating for quantification of cells in FINE and 4iLA+feeder culture conditions after transfection with mCherry-containing plasmid gRNA 2 and staining with an anti-CD75 antibody.

(B) Targeting efficiency for FINE and 4iLA+feeder determined by T7 endonuclease assay. Gel image example from cells transfected with gRNA 2 (left), and quantification of 5 replicates (right).

(C-D) qPCR analysis of naïve-associated transcripts in **(C)** H9 hESCs cultured under mTeSR1, FINE and FINE with low PD03 conditions, and **(D)** in H1 hESCs cultured under FINE (P5 and P24) and mTeSR1. Mean ± SD of three independent experiments.

(E) qPCR analysis of 8-cell-stage-associated transcripts in H1 hESCs cultured under mTeSR1, 4iLA+feeder and FINE conditions. Mean ± SD of two independent experiments.

Table S1 (separate excel file). Z-scores for LTR7Y fluorescence and cell counts for all wells from the high-throughput screen performed to identify compounds supporting feeder-free culture of naïve hESCs, related to Fig. 1.

Table S2. Formulations for the 21 conditions used to optimize feeder-free naïve hESC culture, related to Fig. 2.

Conditions:	Details:
C1	4iLA + Dasatinib 0.2 μM
C2	4iLA + Dasatinib 0.5 μM
C3	4iLA + SRCi
C4	4iLA + Dasatinib 0.5 μM -LIF
C5	4iLA + Dasatinib 0.5 μM - ActivinA
C6	4iLA + Dasatinib 0.5 μM - PD0325901
C7	4iLA + Dasatinib 0.5 μM - SB590885
C8	4iLA + Dasatinib 0.5 μM - bFGF
C9	4iLA + Dasatinib 0.5 μM + CHIR99021 1.0 μM
C10	4iLA + Dasatinib 0.5 μM + PD0325901 0.5 μM
C11	4iLA + Dasatinib 0.5 μM + SB590885 0.25 μM
C12	4iLA + Dasatinib 0.5 μM + PD0325901 0.5 μM + SB590885 0.25 μM
C13	4iLA + Saracatinib 0.5 μM
C14	4iLA + Saracatinib 0.2 μM
C15	4iL + AZD5438 0.2 μM
C16	4iLA + Dasatinib 1.0 μM
C17	4iLA + Dasatinib 2.5 μM
C18	4iLA + Dasatinib 0.5 μM + AZD5438 0.1 μM
C19	4iLA + Dasatinib 0.2 μM + AZD5438 0.2 μM
C20	4iLA + Dasatinib 0.2 μM + AZD5438 0.1 μM
C21	4iLA + Dasatinib 0.5 μM + AZD5438 0.2 μM
4iLA control	4iLA

Table S3. List of antibodies used in this study, related to Experimental Procedures.

Gene name	Company	Catalog number	Application and dilution
OCT4	Abcam	ab19857	IF (1:5000)
NANOG	R&D	AF1997	IF (1:100)
KLF4	Santa Cruz	sc-20691	IF (1:400)
KLF17	Sigma	HPA024629	IF (1:500)
CD75	Abcam	ab77676	IF (1:100)
TFE3	Sigma	HPA023881	IF (1:700)
Ki67	BD Pharmingen	550609	IF (1:300)
H3K9me3	Active Motif	39765	IF (1:500)
CD75 - eFluor 660	eBioscience	50-0759-42	FACS 5ul/test
CD130 - PE	BD Biosciences	555757	FACS 20ul/test

Table S4. Sequences of qPCR primers used in this study, related to Experimental Procedures.

Gene name	Primer sequence Forward	Primer sequence Reverse
POU5F1/OCT4	CTTCGCAAGCCCTCATTTCACCA	GCACTAGCCCCACTCCAACCTG
NANOG	TTCTGCTGAGATGCCTCACACGG	TCTTGACCGGGACCTTGTCTTCC
SOX2	AACCCCAAGATGCACAACTC	CGGGGCCGGTATTTATAATC
PRDM14	GATGGCGCCTCCCTTGCTGA	CGCAGGGGGCGGTGGAATTA
LTR7Y	GCCATTTTATAGGATTTGGGAAG	TAACTGATGACATTCCACCATTG
HERVH	GCCTCTGCTCCTCCACCCTATAA	CGTTTAGCTCCAGCCACCTTTTT
KLF2	CACCAAGAGTTCGCATCTGAAGG	TACATGTGCCGTTTCATGTGCAG
KLF4	CTGGGTCTTGAGGAAGTGCTGAG	GTGGCATGAGCTCTTGGTAATGG
KLF5	TCAGACAGCAGCAATGGACACTC	GTGGCCTGTTGTGGAAGAAACTG
KLF17	GGGATGGTGCGATAGATTCA	GCCTCACCCTCACCTAACAA
DPPA3	ATCGGAAGCTTTACTCCGTCGAG	CCCTTAGGCTCCTTGTTTGTTGG
DPPA5	ACATCGAGCAGGTGAGCAAGG	CATGGCTTCGGCAAGTTTGAG
DNMT3L	CTGCGGAAGTCTCCAGGTTCA	GTAGCATCGGGTGCAATCAGG
GATA2	GGTGCCCATAGTAGCTAGGC	GACAAGGACGGCGTCAAGTA
GATA6	AGCCCAGGCTGCAGTTTTCCG	AGTCAAGGCCATCCACGGTCC
GAPDH	GGCTGTGGGCAAGGTCATCCCTGAG	GTCGCTGTTGAAGTCAGAGGAGACCACCTG
THOC2	GCCACCGGACTTAACCAAGA	CTGTGCTTGTCCGAGGACTT
HUWE1	ACTGGTGCAACTTCCTCCTTC	CCAAGTGCAGCTCCCATTCT
ATRX	ATGTAGGTGGTGTGCGGAAG	ACAGCATCCATCGCTCGAAA
ZSCAN4	CACCAGAGAAGACACAGGAATG	ATGCACCCGTAGGTCTGATA
KDM4E	CAGGGAGGTGTGTTTACTCAAT	GTGTGGCGGAGTCTGATATTT
MBD3L2	AACCTGCGTTCACCTCTTT	GCCATGTGGATTTCTCGTTTC

Table S5. Customised FISH probes, related to Experimental Procedures.

FISH probe	Probe sequence (5' to 3')	Probe sequence (5' to 3')
HUWE1	gaaccagtgagaaacgctgaag	Cataaaggcagatagccaacac
	tatatgcaacgcctagtagtta	Caacggacaagaaacgaggtgg
	aactattgatatttgcctattt	Cagaaaaggtaggggaaagggg
	gtccgttctaatttaaatagtt	Ctcgagaaaaaccagggtattc
	ttttccattctaatgcattgtt	Ctaagccttagctctaaaaccg
	atccaatctggcttgatttgtg	Gaagattagatgggacgacaga
	ccaacagtgtttctccaataaa	Ttaaataccagcctcaactatc
	aagccaccaattttaactactg	Aggacttaggctaaactcgaat
	aaaggccatatcattagttcta	Tatggcaccatccacaaagatg
	acctgaatccatcttaatctaa	Agacttgaggaaatggaaggct
	ctgtctccaggaataacatatt	Cggatcagagtcatacaaacat
	attctggaagcggagcaaagag	Agcagcatgcagagctaagaaa
	aaggctgtaccaattagccaaa	Tcatagtttcgcttaatagtgg
	aaaatgactgggagtttttcgg	Aaactgcaatatccaaacaccg
	ctcctaaaaaggagaaaggcgg	Taatggccgtaaacgaaaaggc
	ggaaacatgagatatcgcgaga	Ggggaggaatgaggaaggcaag
	cttcttaattcaccgcaggatg	Tttactggagagttatcctcta
	cgttgagaactatcgcgatatt	Tcagcagcaaaaatagatgtcc
	cacaacctaacgaagcagtgag	Gaagtgagaagcaggtaagagg
	ctacgcgaagcgaaaagcaaat	Tggaaaaggagtatggggagtg
	aaagccgaagtagctacagctt	Ttatcttccttctaagggattc
	aacctctaccggacgggaaaag	Aaggggtaaaatgtagtggagc
	gagaattctccggcttagaacg	Acaatcaatgctgttttctagt
	aacgaatcccacgaggacgtaa	tgatagggaattaactgcctat

FISH probe	Probe sequence (5’ to 3’)	Probe sequence (5’ to 3’)
XACT	acatccaactacttacagtttc	Ggtactaccattttgaatcatt
	acatacccactttcataatttt	Aaacatgctgctctaagactat
	ttctaacactatttaattgccc	Acttgattatattcagagtttt
	actggaatgatgattgcaatca	Agatcattcaagtaagtctcaa
	atggtattccatgttattcgac	Ggtgttacattatagccaatta
	tctttaaggtgataattcctga	Atctggcagaaactctcattac
	atagcttaaggtactgaaagca	Acacagtgtgttcattataacc
	agttttatagtacttacttggt	Tactcagttactagcttcatta
	tcatttagatggcatccaaaga	Gcaatggattctagtgaaatct
	tttctagctctactttgtgtaa	Tcttaactgggctaccataaaa
	aaagtggcattttcaacctatt	Ctggcagaattctaaactcata
	tttggataatacagcaaatgcc	Tatggtttattaactactgaca
	atttctatgtgttgcagatgag	Agtccttctgattttgtgaaag
	tggcaaataaaggaagctgaca	Cttggacaaatcaacccaggag
	ggaagtcagggtgttaaaatgg	Catgtggatggtcaaagaatct
	ggggactgaaaagtaaacattt	Aaagaaagaacttgccagctgg
	gatgtatgagtagacatagctc	Acaaaaccaggaatagtagaca
	aacagccacttttagttgaatt	Gtagctgaaagtctgggaaaga
	cgttgttttatttcaatgttgt	Ccagaacttatgactgtcaata
	caccgacaaattgttgcaattc	Gaagatatgtggatagcagcat
	ctttaatgttgatggtgctaat	Ttcatgtgagttactctctact
	gtacagttatgagtatatttcc	Ccattaaaactgtccaagtctg
	tgctatgctattctctgaatta	Ttaggatatatacagatatcca

Supplemental Experimental Procedures:

Small molecules treatment

3iL and 4iLA media were supplemented with small molecule compounds at various concentrations for single and combinatory treatments. Small molecules used in the study: Dasatinib (Selleckchem), AZD5438 (TOCRIS), CHIR-98014 (Sigma), Crenolanib (Selleckchem), Saracatinib (Selleckchem), Src Inhibitor-1 (Sigma), Nilotinib (STEMCELL Technologies), Imatinib (STEMCELL Technologies), Dinaciclib (Selleckchem), WH-4-023 (Sigma).

RNA extraction, reverse transcription and qPCR

Total RNA was extracted using TRIzol reagent (Invitrogen) according to manufacturer's protocol followed by DNAase I treatment (Ambion).
250-1000ng of DNAase treated RNA was reverse transcribed using SuperScript II (Invitrogen) and oligo-dT primers (Invitrogen) according to manufacturer's instructions. Reactions were performed in final volume of 20µl. cDNA was diluted before qPCR analysis.
qPCR was performed using KAPA SYBR FAST master mix (KAPA Biosystem) following standard procedures. qPCR reactions were performed in biological duplicates or triplicates in 384-well plates on the ViiA™ 7 Real-Time PCR System (Life Technologies). Two technical replicates were carried out for each qPCR reaction and data was normalised to *GAPDH*. The relative abundance of transcripts was calculated using ΔΔC(T) method. Primer sequences used in this study are listed in Table S3.

RNA-seq analysis

RNA-seq data were mapped against the human genome version hg19 with STAR-2.5.2b (Dobin et al., 2013). R-3.4.1 (R Development Core Team, 2014) and Bioconductor 3.6(Gentleman et al., 2004) were used for the RNA-Seq analysis. Reads were counted using the R package GenomicAlignments (Lawrence et al., 2013) (mode='Union', inter.feature=FALSE), only primary read alignments were retained. Rlog transformed values of the counts, sample normalization factor of the samples, and differential expression values of genes were calculated using DESeq2 (Love et al., 2014). Plots in Figure 4 were created using ggplot2_2.2.1 (Wickham, 2016). Normalized values of repeats were calculated by dividing read counts to both sample normalization factor and per kb of the repeat. For every stages of single cell data, Wilcoxon test is performed against the other stages in order to find the differentially expressed repeats. Afterwards the p-values were corrected by using Benjamini & Hochberg method. Significantly expressed repeats should have at least average 20 RNA-Seq reads in one of the development stages, log 2 change value should be higher than 1 (or lower than -1), and their adjusted p-values should be smaller than 0.05. RNA-seq data have been deposited in GEO under accession number GEO: E-MTAB-8216.

DNA methylation analysis

The resulting raw data were normalized and processed using the ChAMP package under R statistical environment (v.3.1.1). The probes were aligned to the hg19 genome. Percentage of CG methylation was calculated by pooling all probes from individual chromosomes or different categories of genes. Pairwise methylation correlation plot was generated by linear regression model or Lowess weight model using methylation percentage from all probes in the sample. The chromosome and gene methylation track view was generated from Integrative Genomics Viewer (v.2.5.x).

Immunofluorescence
Before fixation with 4% formaldehyde (Sigma) cells were washed with PBS (Gibco) in tissue culture plates (Falcon) for 30 minutes at room temperature. Permeabilization was performed with 1% of Triton-X 100 in PBS followed by blocking step performed in blocking buffer (blocking buffer - 8% FBS in PBS-T (PBS-T 1% Tween in PBS)) each for 30 minutes at room temperature. Cells were incubated with primary antibodies, diluted in blocking buffer, overnight at 4^{o}C with gentle agitation. Primary antibodies details used in the study are provided in Table S4. Cells were washed three times with PBS-T, following 2 hours incubation in room temperature with secondary antibodies (Alexa Fluor-couple, Invitrogen) followed by washes with PBS-T. Nuclei were counterstained with DAPI or Hoechst. After washing three times images were taken using Zeiss Axiovert Epifluorescence microscope. Images were processed using ImageJ and Illustrator. Antibodies used in this study are listed in Table S4.

Virus production
Virus packaging was performed using the third-generation viral packaging system with plasmids: pMDLg/pRRE (Addgene # 12251), pRSV-Rev (Addgene # 12253), pMD2.G (Addgene # 12259). HEK-293T cells were transfected using Lipofectamine2000 (Invitrogen). Briefly, culture medium was changed 8h post-transfection and virus-containing supernatant was collected 30-56h post-transfection. Supernatant was filtered through a 0.45mm filter. Virus was concentrated using filter units following manufacturer's instructions (Amicon Ultra-15 Centrifugal Filter Units). For virus transduction, cells were seeded at 30-40% confluency 16-24 h before infection. Cells were transduced with the lentivirus in the presence of 4 μg/ml Polybrene (Sigma).

FISH:
Cells on 22 x 22mm^2 coverslips were fixed with methacarn fixative (3 absolute methanol : 1 glacial acetic acid) at room temperature for 10mins. The cells were hybridized with custom synthesized Stellaris® RNA FISH probes (Table S5) and Human XIST with Quasar® 570 Dye (Cat nb: SMF-2038-1) (Biosearch Technologies) according to manufacturer instructions for hybridization of adherent cells. Briefly, 1μL of reconstituted FISH probe stock was added to 100μL of hybridization buffer (90μL of Stellaris RNA FISH Hybridization buffer (Biosearch Technologies, cat# SMF-HB1-10) and 10μL of deionized formamide) to make a working RNA FISH probe solution of 125nM. Cells were washed with Wash Buffer A (2mL of Stellaris RNA FISH Wash Buffer A (Biosearch Technologies, cat# SMF-WA1-60), 7mL of nuclease-free water and 1mL of deionized formamide) at room temperature for 5min and incubated with RNA FISH probe solution in the dark at 37°C for 16h. Cells were then transferred to 6 well plate containing fresh Wash Buffer A and incubated in the dark at 37°C for 30min. Wash solution was aspirated and cells were incubated with DAPI nuclear stain (Wash Buffer A containing 5ng/mL DAPI) to counterstain the nuclei in the dark at 37°C for 30min. After that, cells were washed with Wash Buffer B (Biosearch Technologies, cat# SMF-WB1-20) for 5min and then mounted onto glass microscope slides with mounting medium. Images were acquired by the automated slide scanner system (MetaSystems), using classifier MetaCyte SpotCount.Link.Quasar 570-670-63x-BIG. Images were then analyzed using the proprietary software Metafer 4 v3.11.8. A total of 250 cells were captured for each sample. Cells with poor probe hybridization were excluded from analysis and only cells with 2 spot staining present for control RNA FISH probe *XACT* were analyzed.

Teratomas
hESCs were dissociated with TrypLE Express (Life Technologies) and resuspended in 2x matrigel (Corning) diluted in DMEM:F12 (Nacalai Tesque) at the concentration cells 10^6

cells/ml. 200µl of cell suspension was injected into dorsal flanks of SCID nude mice. 4-8 weeks post injection, teratomas were surgically harvested for Mallory's Tetrachome staining. All animal experiments were approved by the A*STAR Institutional Animal Care and Use Committee (IACUC) following the National Advisory Committee for Laboratory Animal Research (NACLAR) Guidelines. All animals were kept in pathogen free conditions in the AAALAC-accredited A*STAR animal facility.

Karyotyping
Various hESCs lines were seeded into glass cover slip slides as single cells. Karyotyping service including colcemid treatment and G-band analysis was outsourced with Parkway Laboratory Services.

RA differentiation
mTeSR1 (STEMCELL Technologies) medium was supplemented with retinoic acid (Sigma, 10 µM) to induce exit from pluripotent state. Medium was refreshed daily. Cells were lysed for RNA work or FACS analysis 4 days after treatment.

Flow cytometry analysis
LTR7Y-ZsGreen, mTeSR1, 4iLA + feeder and FINE cells were dissociated with TrypLE and resuspended as single cells in staining solution (2% FBS in PBS) with Thiazovivin (1 µM). Staining with CD75 and CD130 (Table S4) was performed on ice for 30min followed by washes. Fluorescence intensity was analysed on BD LSRFortessa. FACS analysis was performed using FlowJo software.

CRISPR/Cas9 targeting
Transfection of mTeSR1, FINE and 4iLA+feeders cells with single plasmid co-expressing Cas9, gRNA and mCherry (GeneArt CRISPR EF1a-SpCas9-mCherry+gRNA) was performed using Mirus *Trans*IT-LT1 (MirusBio). CRISPR/gRNA plasmids are gift from Meng How Tan laboratory. Cells were FACS sorted using BD FACS Aria II 48h post-transfection for mCherry positive cells. DNA for PCR was extracted from sorted cells using QuickExtract (Epicentre) according to manufacturer's protocol. Genes targeted: *EGFR* (gRNA 1) and *STAG2* (gRNA 2) protocol. Quantification was performed as previously described in (Ran et al., 2013). For T7 assay, PCR for T7 endonuclease assay was performed using Q5 High-Fidelity DNA Polymerase (NEB) with primers spanning region targeted by gRNA. T7 assay was performed according to manufacturer's protocol.

References

Araujo, J., and Logothetis, C. (2010). Dasatinib: a potent SRC inhibitor in clinical development for the treatment of solid tumors. Cancer Treat Rev 36, 492-500.

Barakat, T.S., Halbritter, F., Zhang, M., Rendeiro, A.F., Perenthaler, E., Bock, C., and Chambers, I. (2018). Functional Dissection of the Enhancer Repertoire in Human Embryonic Stem Cells. Cell Stem Cell 23, 276-288 e278.

Betschinger, J., Nichols, J., Dietmann, S., Corrin, P.D., Paddison, P.J., and Smith, A. (2013). Exit from Pluripotency Is Gated by Intracellular Redistribution of the bHLH Transcription Factor Tfe3. Cell 153, 335-347.

Brons, I.G., Smithers, L.E., Trotter, M.W., Rugg-Gunn, P., Sun, B., Chuva de Sousa Lopes, S.M., Howlett, S.K., Clarkson, A., Ahrlund-Richter, L., Pedersen, R.A., et al. (2007). Derivation of pluripotent epiblast stem cells from mammalian embryos. Nature 448, 191-195.

Chambers, I., Silva, J., Colby, D., Nichols, J., Nijmeijer, B., Robertson, M., Vrana, J., Jones, K., Grotewold, L., and Smith, A. (2007). Nanog safeguards pluripotency and mediates germline development. Nature 450, 1230-1234.

Chan, Y.S., Goke, J., Ng, J.H., Lu, X., Gonzales, K.A., Tan, C.P., Tng, W.Q., Hong, Z.Z., Lim, Y.S., and Ng, H.H. (2013). Induction of a human pluripotent state with distinct regulatory circuitry that resembles preimplantation epiblast. Cell Stem Cell 13, 663-675.

Di Stefano, B., Ueda, M., Sabri, S., Brumbaugh, J., Huebner, A.J., Sahakyan, A., Clement, K., Clowers, K.J., Erickson, A.R., Shioda, K., et al. (2018). Reduced MEK inhibition preserves genomic stability in naive human embryonic stem cells. Nat Methods 15, 732-740.

Dobin, A., Davis, C.A., Schlesinger, F., Drenkow, J., Zaleski, C., Jha, S., Batut, P., Chaisson, M., and Gingeras, T.R. (2013). STAR: ultrafast universal RNA-seq aligner. Bioinformatics *29*, 15-21.

Eot-Houllier, G., Fulcrand, G., Magnaghi-Jaulin, L., and Jaulin, C. (2009). Histone deacetylase inhibitors and genomic instability. Cancer Lett 274, 169-176.

Evans, M.J., and Kaufman, M.H. (1981). Establishment in culture of pluripotential cells from mouse embryos. Nature 292, 154-156.

Gafni, O., Weinberger, L., Mansour, A.A., Manor, Y.S., Chomsky, E., Ben-Yosef, D., Kalma, Y., Viukov, S., Maza, I., Zviran, A., et al. (2013). Derivation of novel human ground state naive pluripotent stem cells. Nature 504, 282-286.

Gardner, R.L. (1998). Contributions of blastocyst micromanipulation to the study of mammalian development. Bioessays 20, 168-180.

Gardner, R.L., and Beddington, R.S. (1988). Multi-lineage 'stem' cells in the mammalian embryo. J Cell Sci Suppl 10, 11-27.

Gentleman, R.C., Carey, V.J., Bates, D.M., Bolstad, B., Dettling, M., Dudoit, S., Ellis, B., Gautier, L., Ge, Y., Gentry, J., *et al.* (2004). Bioconductor: open software development for computational biology and bioinformatics. Genome Biol *5*, R80.

Goke, J., Lu, X., Chan, Y.S., Ng, H.H., Ly, L.H., Sachs, F., and Szczerbinska, I. (2015). Dynamic transcription of distinct classes of endogenous retroviral elements marks specific populations of early human embryonic cells. Cell Stem Cell 16, 135-141.

Gonzales, K.A., Liang, H., Lim, Y.S., Chan, Y.S., Yeo, J.C., Tan, C.P., Gao, B., Le, B., Tan, Z.Y., Low, K.Y., et al. (2015). Deterministic Restriction on Pluripotent State Dissolution by Cell-Cycle Pathways. Cell 162, 564-579.

Grow, E.J., Flynn, R.A., Chavez, S.L., Bayless, N.L., Wossidlo, M., Wesche, D.J., Martin, L., Ware, C.B., Blish, C.A., Chang, H.Y., et al. (2015). Intrinsic retroviral reactivation in human preimplantation embryos and pluripotent cells. Nature 522, 221-225.

Guo, G., von Meyenn, F., Rostovskaya, M., Clarke, J., Dietmann, S., Baker, D., Sahakyan, A., Myers, S., Bertone, P., Reik, W., et al. (2017). Epigenetic resetting of human pluripotency. Development 144, 2748-2763.

Hayashi, K., Lopes, S.M., Tang, F., and Surani, M.A. (2008). Dynamic equilibrium and heterogeneity of mouse pluripotent stem cells with distinct functional and epigenetic states. Cell Stem Cell 3, 391-401.

Lawrence, M., Huber, W., Pages, H., Aboyoun, P., Carlson, M., Gentleman, R., Morgan, M.T., and Carey, V.J. (2013). Software for computing and annotating genomic ranges. PLoS Comput Biol *9*, e1003118.

Li, J., Rix, U., Fang, B., Bai, Y., Edwards, A., Colinge, J., Bennett, K.L., Gao, J., Song, L., Eschrich, S., et al. (2010). A chemical and phosphoproteomic characterization of dasatinib action in lung cancer. Nat Chem Biol 6, 291-299.

Lin, H., Gupta, V., Vermilyea, M.D., Falciani, F., Lee, J.T., O'Neill, L.P., and Turner, B.M. (2007). Dosage compensation in the mouse balances up-regulation and silencing of X-linked genes. PLoS Biol 5, e326.

Love, M.I., Huber, W., and Anders, S. (2014). Moderated estimation of fold change and dispersion for RNA-seq data with DESeq2. Genome Biol *15*, 550.

Lu, X., Sachs, F., Ramsay, L., Jacques, P.E., Goke, J., Bourque, G., and Ng, H.H. (2014). The retrovirus HERVH is a long noncoding RNA required for human embryonic stem cell identity. Nat Struct Mol Biol 21, 423-425.

Macfarlan, T.S., Gifford, W.D., Driscoll, S., Lettieri, K., Rowe, H.M., Bonanomi, D., Firth, A., Singer, O., Trono, D., and Pfaff, S.L. (2012). Embryonic stem cell potency fluctuates with endogenous retrovirus activity. Nature 487, 57-63.

Martello, G., Sugimoto, T., Diamanti, E., Joshi, A., Hannah, R., Ohtsuka, S., Gottgens, B., Niwa, H., and Smith, A. (2012). Esrrb is a pivotal target of the gsk3/tcf3 axis regulating embryonic stem cell self-renewal. Cell Stem Cell 11, 491-504.

Martin, G.R. (1981). Isolation of a pluripotent cell line from early mouse embryos cultured in medium conditioned by teratocarcinoma stem cells. Proc Natl Acad Sci U S A 78, 7634-7638.

Nakamura, T., Okamoto, I., Sasaki, K., Yabuta, Y., Iwatani, C., Tsuchiya, H., Seita, Y., Nakamura, S., Yamamoto, T., and Saitou, M. (2016). A developmental coordinate of pluripotency among mice, monkeys and humans. Nature 537, 57-62.

Nichols, J., and Smith, A. (2009). Naive and primed pluripotent states. Cell Stem Cell 4, 487-492.

Nishizawa, M., Chonabayashi, K., Nomura, M., Tanaka, A., Nakamura, M., Inagaki, A., Nishikawa, M., Takei, I., Oishi, A., Tanabe, K., et al. (2016). Epigenetic Variation between Human Induced Pluripotent Stem Cell Lines Is an Indicator of Differentiation Capacity. Cell Stem Cell 19, 341-354.

Niwa, H., Ogawa, K., Shimosato, D., and Adachi, K. (2009). A parallel circuit of LIF signalling pathways maintains pluripotency of mouse ES cells. Nature 460, 118-122.

R Development Core Team (2014). R: A language and environment for statistical computing (Vienna, Austria: R Foundation for Statistical Computing).

Ran, F.A., Hsu, P.D., Wright, J., Agarwala, V., Scott, D.A., and Zhang, F. (2013). Genome engineering using the CRISPR-Cas9 system. Nat Protoc *8*, 2281-2308.

Reubinoff, B.E., Pera, M.F., Fong, C.Y., Trounson, A., and Bongso, A. (2000). Embryonic stem cell lines from human blastocysts: somatic differentiation in vitro. Nat Biotechnol 18, 399-404.

Sahakyan, A., Kim, R., Chronis, C., Sabri, S., Bonora, G., Theunissen, T.W., Kuoy, E., Langerman, J., Clark, A.T., Jaenisch, R., et al. (2017). Human Naive Pluripotent Stem Cells Model X Chromosome Dampening and X Inactivation. Cell Stem Cell 20, 87-101.

Takashima, Y., Guo, G., Loos, R., Nichols, J., Ficz, G., Krueger, F., Oxley, D., Santos, F., Clarke, J., Mansfield, W., et al. (2014). Resetting transcription factor control circuitry toward ground-state pluripotency in human. Cell 158, 1254-1269.

Tesar, P.J., Chenoweth, J.G., Brook, F.A., Davies, T.J., Evans, E.P., Mack, D.L., Gardner, R.L., and McKay, R.D. (2007). New cell lines from mouse epiblast share defining features with human embryonic stem cells. Nature 448, 196-199.

Theunissen, T.W., Friedli, M., He, Y., Planet, E., O'Neil, R.C., Markoulaki, S., Pontis, J., Wang, H., Iouranova, A., Imbeault, M., et al. (2016). Molecular Criteria for Defining the Naive Human Pluripotent State. Cell Stem Cell 19, 502-515.

Theunissen, T.W., Powell, B.E., Wang, H., Mitalipova, M., Faddah, D.A., Reddy, J., Fan, Z.P., Maetzel, D., Ganz, K., Shi, L., et al. (2014). Systematic identification of culture conditions for induction and maintenance of naive human pluripotency. Cell Stem Cell 15, 471-487.

Thomson, J.A., Itskovitz-Eldor, J., Shapiro, S.S., Waknitz, M.A., Swiergiel, J.J., Marshall, V.S., and Jones, J.M. (1998). Embryonic stem cell lines derived from human blastocysts. Science 282, 1145-1147.

Torres-Padilla, M.E., and Chambers, I. (2014). Transcription factor heterogeneity in pluripotent stem cells: a stochastic advantage. Development 141, 2173-2181.

Tosolini, M., Brochard, V., Adenot, P., Chebrout, M., Grillo, G., Navia, V., Beaujean, N., Francastel, C., Bonnet-Garnier, A., and Jouneau, A. (2018). Contrasting epigenetic states of heterochromatin in the different types of mouse pluripotent stem cells. Sci Rep 8, 5776.

van den Berg, D.L., Zhang, W., Yates, A., Engelen, E., Takacs, K., Bezstarosti, K., Demmers, J., Chambers, I., and Poot, R.A. (2008). Estrogen-related receptor beta interacts with Oct4 to positively regulate Nanog gene expression. Mol Cell Biol 28, 5986-5995.

Ware, C.B. (2017). Concise Review: Lessons from Naive Human Pluripotent Cells. Stem Cells 35, 35-41.

Ware, C.B., Nelson, A.M., Mecham, B., Hesson, J., Zhou, W., Jonlin, E.C., Jimenez-Caliani, A.J., Deng, X., Cavanaugh, C., Cook, S., et al. (2014). Derivation of naive human embryonic stem cells. Proc Natl Acad Sci U S A 111, 4484-4489.

Weinberger, L., Ayyash, M., Novershtern, N., and Hanna, J.H. (2016). Dynamic stem cell states: naive to primed pluripotency in rodents and humans. Nat Rev Mol Cell Biol 17, 155-169.

Wickham, H. (2016). Ggplot2 - elegant graphics for data analysis.

Xue, Z., Huang, K., Cai, C., Cai, L., Jiang, C.Y., Feng, Y., Liu, Z., Zeng, Q., Cheng, L., Sun, Y.E., et al. (2013). Genetic programs in human and mouse early embryos revealed by single-cell RNA sequencing. Nature 500, 593-597.

Yan, L., Yang, M., Guo, H., Yang, L., Wu, J., Li, R., Liu, P., Lian, Y., Zheng, X., Yan, J., et al. (2013). Single-cell RNA-Seq profiling of human preimplantation embryos and embryonic stem cells. Nat Struct Mol Biol 20, 1131-1139.

Ying, Q.L., Wray, J., Nichols, J., Batlle-Morera, L., Doble, B., Woodgett, J., Cohen, P., and Smith, A. (2008). The ground state of embryonic stem cell self-renewal. Nature 453, 519-523.

Zernicka-Goetz, M., Morris, S.A., and Bruce, A.W. (2009). Making a firm decision: multifaceted regulation of cell fate in the early mouse embryo. Nat Rev Genet 10, 467-477.